AlGaN-Based Vertical Injection Laser Diodes Using Inverse Tapered p-Waveguide for Efficient Hole Transport

Md. Mahbub Satter, Zachary Lochner, *Student Member, IEEE*, Tsung-Ting Kao, Yuh-Shiuan Liu, Xiao-Hang Li, Shyh-Chiang Shen, *Senior Member, IEEE*, Russell D. Dupuis, *Fellow, IEEE*, and P. D. Yoder, *Senior Member, IEEE*

***Abstract*— An AlGaN deep ultraviolet laser diode design exploiting AlN substrates is presented, featuring an inverse-tapered p-waveguide layer. The 2-D optoelectronic simulation predicts lasing at 290 nm. Spatial balancing of the lasing mode to minimize optical loss in the p-Ohmic metallization is achieved through the use of a narrow bandgap yet transparent n-waveguide layer. Several electron blocking layer (EBL) designs are investigated and compared with a conventionally tapered EBL design. Through judicious volumetric redistribution of fixed negative polarization charge, inverse tapering may be exploited to achieve nearly flat valence band profiles free from barriers to hole injection into the active region, in contrast to conventional designs. Furthermore, proper selection of quantum well barrier and spacer compositions are demonstrated to reduce electron leakage from the active region. Numerical simulations demonstrate that the inverse tapered strategy is a viable solution for efficient hole injection in deep ultraviolet laser diodes operating at shorter wavelengths (<290 nm).**

***Index Terms*— AlN substrate, AlGaN epitaxial layer, deep ultraviolet laser diodes, efficient hole transport, hole blocking layer, inverse tapering, optical absorption loss, polarization charge.**

I. Introduction

ULTRAVIOLET (UV) laser diodes (LDs) and light emitting diodes (LEDs) based on the wurtzite III-nitride material system fit the technological needs for a diverse list of present and future applications [1], [2]. Recently, they have been the focus of intense investigation by several photonic device research groups [3]–[10]. The design of vertical injection edge emitting LDs with stimulated emission in the UV-B (280-320 nm) and UV-C (< 280 nm) bands is fraught with numerous complications. A discussion of these issues may be found in the literature [2] and [11]. Among the most serious challenges is inefficient hole injection. The low conductivity of p-type III-nitride material is primarily responsible for this issue. With increasing bandgap energy, the activation energy of Mg dopants [12]–[15] in materials required for DUV LDs increases commensurately, exacerbating the situation. In addition to greater Joule heating in the resistive p-type layers, weak electrical activation of Mg dopants leads to unscreened polarization charge at the interfaces between waveguide and electron blocking layers (EBLs), as well as between spacer and QW layers which in turn contributes electrostatically to the emergence of parasitic hole blocking layers. As the unscreened polarization charge is of positive sign at the spacer/EBL interface, it contributes electrostatically to the emergence of a parasitic hole blocking layer, in which case hole injection into the active region is limited by thermionic emission, and therefore extremely inefficient. Heavily doped p-type layers can only partially suppress such unintentional hole blocking layers, and do so at the expense of degraded hole mobility and material quality. Although narrower bandgap III-nitride materials offer higher p-type conductivity by virtue of a lower Mg activation energy [12]–[15], two considerations preclude their use as p-type layers in DUV LDs. The problems of hole injection and optical confinement are tightly coupled in vertical injection DUV LDs, and the use of narrower bandgap III-nitride materials for p-type layers may shift the optical mode profile upwards towards (high refractive index) p-type layers. This in turn degrades optical confinement and introduces optical absorption losses in both the p-type layers and p-Ohmic metal.

This article presents a 290 nm UV edge emitting vertical injection LD design based exclusively on metal-face growth of ternary AlGaN layers on a bulk *c*-axis AlN substrate. In order to reduce the problem of hole injection, several EBL designs are investigated and compared via numerical simulation. In this article, we suggest that superior hole injection can be achieved if a conventionally tapered EBL [2], [11], [16]–[19] is replaced by an inverse tapered p-waveguide layer whose bandgap decreases along the growth direction. This inverse tapering eliminates the aforementioned electrostatically induced artificial hole blocking layer, and leads to significantly lower threshold current. The design presented here assumes realistic chemical and electrical concentrations of dopant atoms for all p-type layers, and uses ternary AlGaN mole compositions that are feasible with current growth technology. LD designs

Manuscript received September 13, 2013; revised December 6, 2013 and December 30, 2013; accepted January 12, 2014. Date of publication January 20, 2014; date of current version February 5, 2014. This work was supported by the Defense Advanced Research Projects Agency under Contract FA2386-10-1-4152.

The authors are with the School of Electrical and Computer Engineering, Georgia Institute of Technology, Atlanta, GA 30332 USA (e-mail: mmsatter@gatech.edu).

Digital Object Identifier 10.1109/JQE.2014.2300757

TABLE I
EPITAXIAL LAYER STRUCTURE FOR AN AlGaN/AlGaN EDGE EMITTING VERTICAL INJECTION LD DESIGN OPERATING AT 290 nm

Layer Name	Material	Thickness (nm)	Refractive index
Contact	GaN	10	2.603
p-waveguide	$Al_{0.48}GaN$	500	2.624
EBL	$Al_{0.54\text{ - }0.60}GaN$	20	2.565 - 2.522
Spacer	$Al_{0.54}GaN$	5.0	2.565
QW (×2)	$Al_{0.34}GaN$	2.0	2.741
QWB (×2)	$Al_{0.54}GaN$	5.0	2.565
Grading	$Al_{0.45\text{ - }0.54}GaN$	20	2.662 - 2.565
n-waveguide	$Al_{0.45}GaN$	150	2.662
Grading	$Al_{0.70\text{ - }0.45}GaN$	400	2.46 - 2.662
Buffer	$Al_{1.00\text{ - }0.70}GaN$	1000	2.292 - 2.46
Substrate	AlN	-	2.292

targeting shorter emission wavelengths (<290 nm) can easily adopt this idea of inverse tapering and thereby eliminate the severe problem of hole injection.

II. SIMULATION METHOD

A detailed description of our simulation method can be found in previous publications [2], [11], and [20]. Simulation results presented in this article consider the composition-dependence of dopant activation energy [12]–[15], even in graded material, for accurate calculation of incomplete ionization of dopant species [21] throughout the epitaxial layer structure. For the DUV LD designs we propose in the present article, the complexity introduced by this ionization model is critical for the accurate prediction of hole injection. Also, a composition, strain and wavelength dependent complex refractive index model [22], [23] has been used to calculate optical modes and absorption coefficients (and loss) of ternary AlGaN epitaxial layers at the emission wavelength.

III. RESULT

Previously, we have reported AlInN/AlInN [11] and AlGaN/AlInGaN [2] edge emitting LD designs operating at 250 nm wavelength. Our earlier investigations revealed that compositionally graded EBL [11] and polarization charge matched quantum well barriers (QWBs) [2] can significantly improve LD performance. In this article, we seek to improve hole injection through electrostatic engineering of the hole injection layers.

A. Epitaxial Structure Design

To achieve superior hole injection efficiency and minimum optical loss in the p-Ohmic metal, we have explored different p-waveguide layer and EBL designs by means of numerical simulation. Table I lists the epitaxial layer structure of a typical AlGaN/AlGaN edge emitting vertical injection LD design with a conventionally tapered EBL. It is assumed that all layers are pseudomorphically grown [2], [11] on top of an AlN substrate. 500 μm edge emitting LD stripes are formed by etching to a depth of 310 nm, or 220 nm above the top surface of the spacer, with lasing at $\lambda = 290$ nm. The ridge width is 2 μm and cavity length is 500 μm. Left and right facet reflectivities are assumed to be 85% and 95%

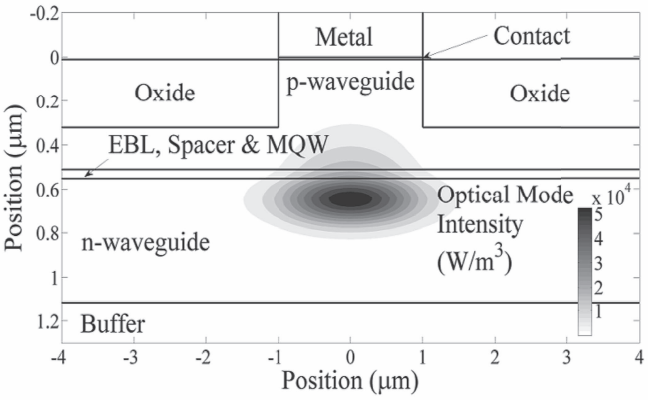

Fig. 1. Optical mode profile corresponding to the epitaxial structure of Table I (Only the lasing TE mode is shown here).

respectively (Mirror loss is 2.14 cm^{-1}). We have considered several TE and TM modes in all simulations, and confirmed that only the fundamental modes are strongly confined by the optical waveguide. Of the two fundamental modes, lasing occurs only in the TE mode over the range of injection currents we have studied, as is expected in compressively strained AlGaN based MQW LD designs [2], [11]. Its optical mode profile is shown in Fig. 1. Refractive indices used for optical mode calculations are presented in Table I, and are estimated from the real part of a complex refractive index model [22], [23]. The imaginary part of this model is used to estimate the absorption coefficients in the epitaxial layers. Except for the QWs, the entire epitaxial structure of Table I is assumed to be optically transparent at the emission wavelength (290 nm). We address the influence of optical loss associated with sub-bandgap absorption [24] at the end of Section III, and stress that the asymmetric waveguide design presented in Table I minimizes such deleterious effects by pushing the optical mode towards less lossy n-type layers [25], [26].

Optical loss in metals plays a critical role in determining the threshold current. For purposes of our numerical calculation, the p- and n-Ohmic metals are taken to be nickel and aluminum, respectively. At $\lambda = 290$ nm, the absorption coefficient of nickel is 8.77×10^5 cm^{-1} and that of aluminum is 1.49×10^6 cm^{-1} [27], resulting in a total optical loss of 2.4 cm^{-1} in the metals for the lasing mode of Fig. 1. Fig. 2 illustrates the energy band diagram at a bias condition below the lasing threshold. L-I and V-I curves are shown in Fig. 3. The threshold current is 715 mA and the slope efficiency is 0.08 W/A. Shockley–Read–Hall lifetime and Auger recombination coefficients, which also strongly influence threshold current, are taken from [28] and [29], respectively. Other parameters used in our calculations have been previously reported [2], [11].

In contrast to previously reported designs [2] and [11], the epitaxial layer structure of Table I exhibits several new features. It only employs ternary AlGaN compositions and avoids ternary AlInN and quaternary AlInGaN. Although AlInN and AlInGaN based designs may offer promising LD performance advantages [2], [11], high quality crystal growth of In-rich materials is presently considered more challenging. In order to achieve higher p-type conductivity, narrow bandgap

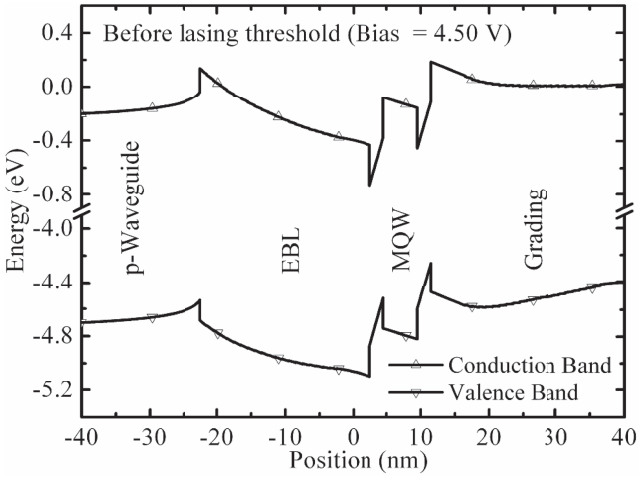

Fig. 2. Energy band diagram of the epitaxial structure of Table I at a bias before the lasing threshold. Conventionally tapered EBL is also acting as a significant hole blocking layer (Barrier height is 0.6 eV).

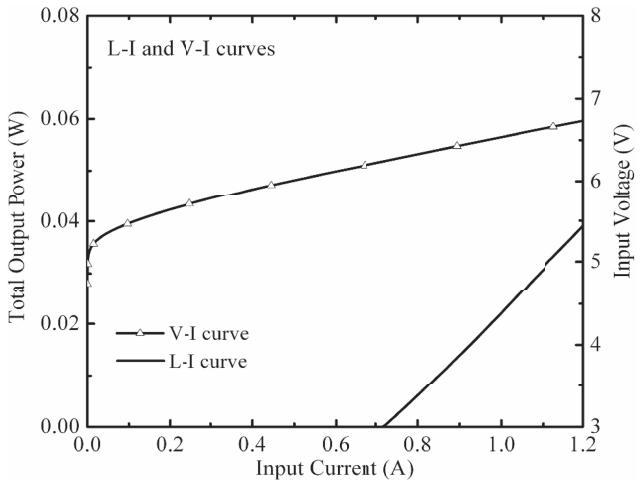

Fig. 3. L-I and V-I curve of the epitaxial structure of Table I.

$Al_{0.48}GaN$ (E_{gap} = 4.58 eV) is utilized for the p-waveguide layer. Wider bandgap material would incur greater Joule heating because of poor p-type conductivity. On the other hand, narrow bandgap p-waveguide material may become optically absorptive at the lasing wavelength, and will moreover exacerbate optical losses by pulling the optical mode towards the highly absorptive p-Ohmic metal.

Similarly, a thinner p-waveguide layer would yield higher optical loss, while a thicker layer would introduce additional series resistance and associated Joule heating. In contrast to previously reported designs [2] and [11], the optical mode profile of devices presented in this article is no longer centered on the active region (See Fig. 1). A narrow bandgap ($Al_{0.45}GaN$) n-waveguide layer is employed to counterbalance the high refractive index of the proposed p-waveguide layer, and to pull the optical mode downwards, away from the lossy p-Ohmic metal. The optical confinement factor is 0.75%. In fact, $Al_{0.45}GaN$ (used for n-waveguide layer) is the smallest possible bandgap material which is transparent at the 290 nm emission wavelength. Thicker and narrower bandgap n-waveguide material may reduce lateral series resistance (and Joule heating) but it would significantly degrade the optical confinement factor and may also introduce additional optical absorption. Furthermore, a thinner and/or wider AlGaN n-waveguide layer may not be able to pull the optical mode downwards effectively if thinner and wider bandgap AlGaN is employed.

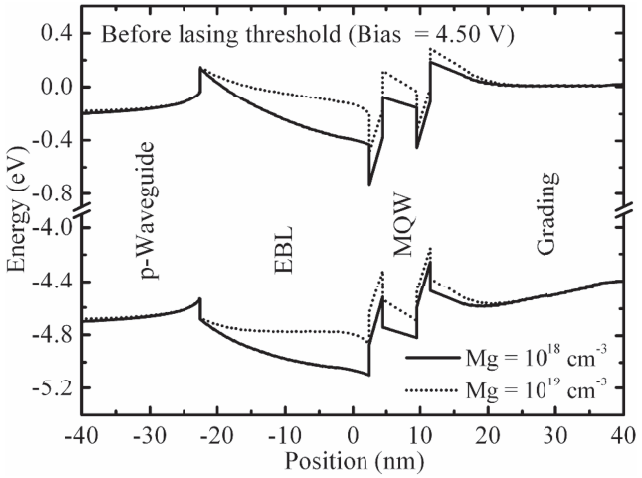

Fig. 4. Effect of heavy Mg doping on the energy band diagram of the epitaxial structure of Table I. Hole blocking layer is suppressed significantly.

From the energy band diagram of Fig. 2, one may observe that a conventionally tapered EBL (in which the bandgap increases along the growth direction) acts as a large hole blocking layer primarily due to the unscreened polarization charge at the p-waveguide layer/EBL and spacer/QW interfaces. The substitutional dopant (Mg) concentration of the spacer, EBL and p-waveguide layer is taken to be 10^{18} cm^{-3} (For the n-waveguide layer, the substitutional Si concentration is assumed to be 2×10^{18} cm^{-3}). We point out that the prominence of this hole blocking layer will be artificially but only partially masked if 100% ionization of dopant atoms is assumed; however, this is not only incorrect, but also leads to a gross overestimate of hole injection efficiency. One way to reduce the potential barrier for hole injection is to dope the p-type layers heavily. Fig. 4 shows the effect of heavy Mg doping on the energy band diagram. As expected, the barrier height of the hole blocking layer is reduced significantly. Both threshold current and voltage are lowered due to improved hole injection efficiency (see Fig. 5). Although heavy doping degrades carrier mobility [30]–[32], this effect alone does not exert a large influence on either threshold current or voltage. Instead, it is the energetic barrier to hole injection due to the valence band discontinuity at the p-waveguide layer/EBL interface with conventional tapering which is the dominant effect, limiting the mechanism for hole injection to mere thermionic emission.

B. Two-Step Tapered EBL Design

The abrupt valence band discontinuity at the p-waveguide layer/EBL interface can be eliminated by using an EBL with two step tapering. Specifically, the bottom half of the EBL may be tapered upwards such that its bandgap increases in the growth direction (from $Al_{0.54}GaN$ to $Al_{0.60}GaN$) for efficient electron blocking. The upper half may be tapered downwards

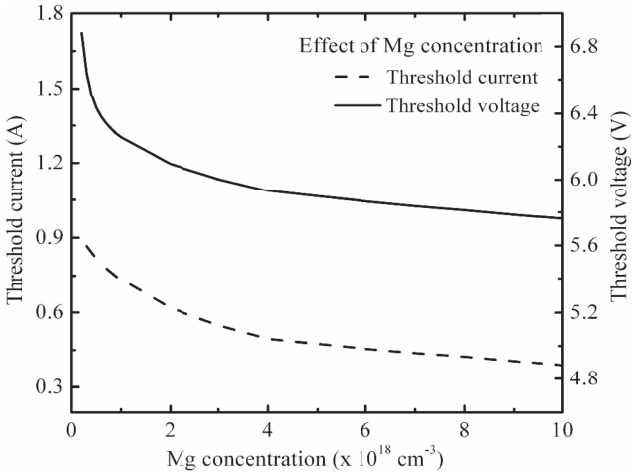

Fig. 5. Both threshold current and voltage improve with heavy doping of p-type layers. But the improvements may be exaggerated because mobility degradation has not been considered explicitly.

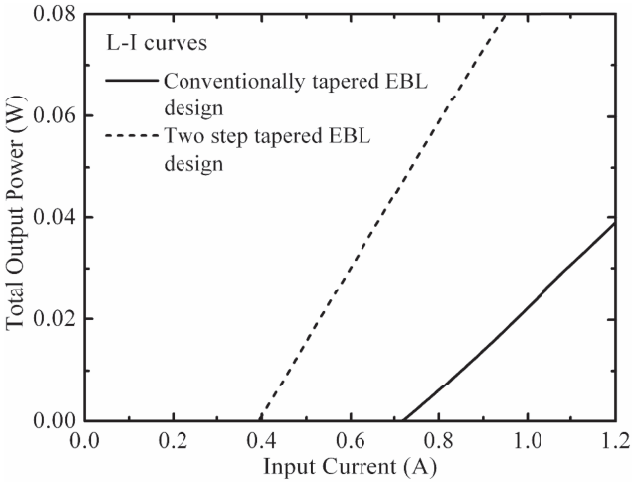

Fig. 7. Comparison of L-I curves between conventionally tapered and two step tapered EBL designs. With two step tapering, threshold current is reduced by 46% and slope efficiency is improved by 76%.

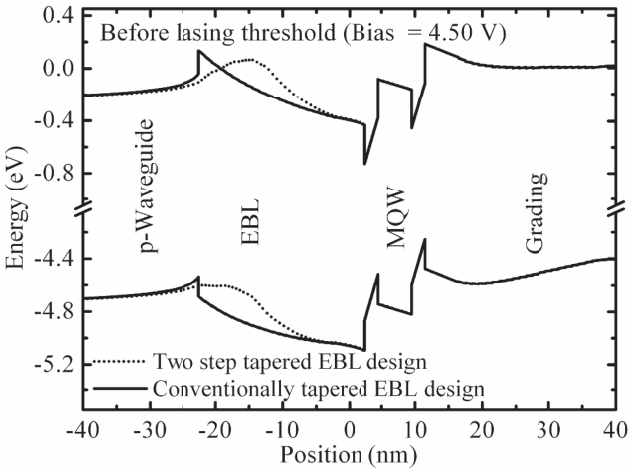

Fig. 6. Comparison of the energy band diagrams between conventionally tapered and two step tapered EBL designs. Two step tapering eliminates the abrupt valence band offset at the p-waveguide layer/EBL interface and reduces the effective thickness of the hole blocking layer.

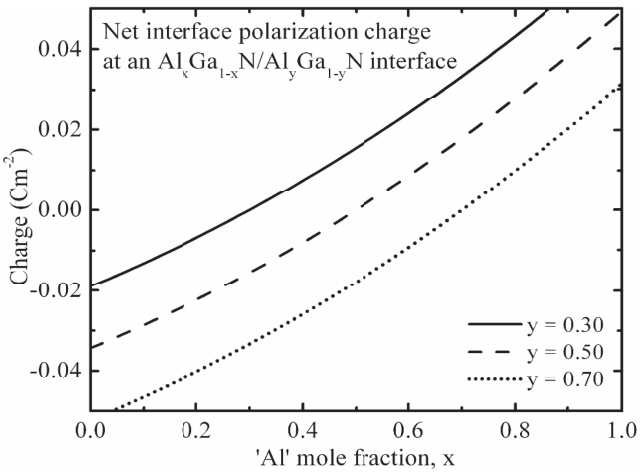

Fig. 8. Compositional dependence of the net interface polarization charge at an AlGaN/AlGaN interface. It is assumed that the layers are pseudomorphically grown on top of AlN substrate.

along the direction of growth (from $Al_{0.60}GaN$ to $Al_{0.48}GaN$) to eliminate abrupt valence band discontinuities. We have simulated the baseline epitaxial structure of Table I by replacing the conventionally tapered EBL with the proposed two step tapered design, and the results are shown in Figs. 6 and 7. For meaningful comparison, the EBL thickness is held constant at 20 nm. Two step tapering of the EBL yields a 46% reduction in threshold current and 76% improvement in slope efficiency (see Fig. 7). Unfortunately, the band diagram of Fig. 6 clearly indicates that the two step tapered EBL does not reduce the size of the potential barrier to hole injection, but merely halves its effective thickness and eliminates the abrupt valence band offset. To improve the hole injection efficiency further, it is important to investigate and understand the nature of this polarization charge induced hole blocking layer in more detail.

The sign and magnitude of the net interface polarization charge of an $Al_xGa_{1-x}N/Al_yGa_{1-y}N$ interface depends on several factors, including growth axis, metal-face vs. N-face growth, difference between mole fraction x and y and their relative significance [22]. In our simulation, metal-face *c*-axis growth is assumed. It is obvious that a large mole fraction contrast will increase the magnitude of the net interface charge, but it is the sign of the difference between x and y which determines the sign of the polarization charge. If we assume that a layer of $Al_xGa_{1-x}N$ is grown on top of $Al_yGa_{1-y}N$, the net interface polarization charge will be positive if $x > y$ and vice versa (see Fig. 8). Therefore, the volumetrically redistributed polarization charge of the two step tapered EBL is positive in the bottom half and negative in the upper half. With moderate dopant (Mg) concentration in the p-type layers (10^{18} cm^{-3}), this redistributed polarization charge opposes the bound charges associated with dopant atoms at the bottom half of EBL and reinforces at the top. In cases where the magnitude of the redistributed polarization charge in the lower half of the EBL exceeds the charge of electrically active dopant atoms in that layer, the location of the p-n junction itself is transferred to the interface between the two halves of the EBL. This explains why the effective thickness of the hole blocking

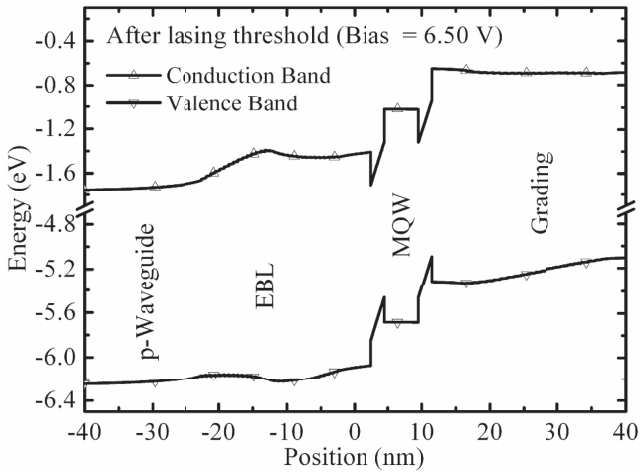

Fig. 9. Energy band diagram of the two step tapered EBL design above lasing threshold. A large fraction of the applied voltage drops across the EBL and makes the conduction band almost flat.

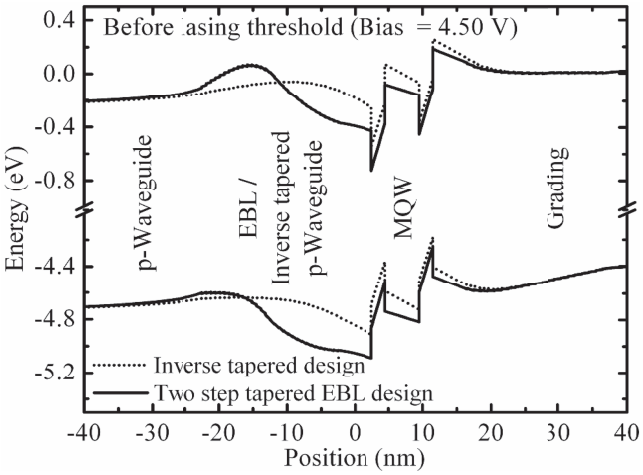

Fig. 10. Comparison of the energy band diagrams between two step tapered EBL and inverse tapered designs. Inverse tapering reduces the potential barrier of the hole blocking layer by 180 meV.

layer is halved in a two step tapered EBL design. Because the volumetric redistribution of polarization charge in the upper half contributes additively to the fixed charge contributed by ionized Mg atoms, the potential drop over the EBL layer is primarily across the bottom half, while the valence band is almost flat throughout the upper half (see Fig. 6).

C. Inverse Tapered p-Waveguide Design

Now that the root cause of the hole blocking layer has been identified, the next step is to address strategies for its suppression. One such approach is to flip the sign of the polarization charge at the bottom half of two step tapered EBL, in such a way that the redistributed polarization charge should be negative throughout the entire thickness of the EBL. From a compositional perspective, this means that the two step tapered EBL should be replaced by an inverse tapered p-waveguide layer where the bandgap should decrease along the growth direction. This may be a risky proposition, as electrons may leak from the MQW active region in the absence of an explicit EBL, and thereby degrade LD performance. However, in spite of the band diagram under flatband conditions, our numerical simulations reveal that above the lasing threshold, neither the conventional nor the two step tapered EBL are effective in blocking electrons anyway, due to the redistribution of electrostatic potential under strong forward bias. Indeed, because of poor p-type conductivity, a large fraction of the applied voltage is dropped across the EBL. This point is demonstrated in Fig. 9. Above the lasing threshold, the conduction band is almost flat at the bottom half of the two step tapered EBL, and the only thing impeding the leakage of electrons is the conduction band offset at the spacer/QW interface. Nevertheless, in spite of electron leakage, numerical simulations indicate that this device can be made to lase, albeit at high injection current density. A similar result is observed for the conventionally tapered EBL (results not shown here). This observation suggests that the inverse tapering efficacy in DUV LD design may actually solve the problem of poor hole injection. Still, care must be taken to keep the electron

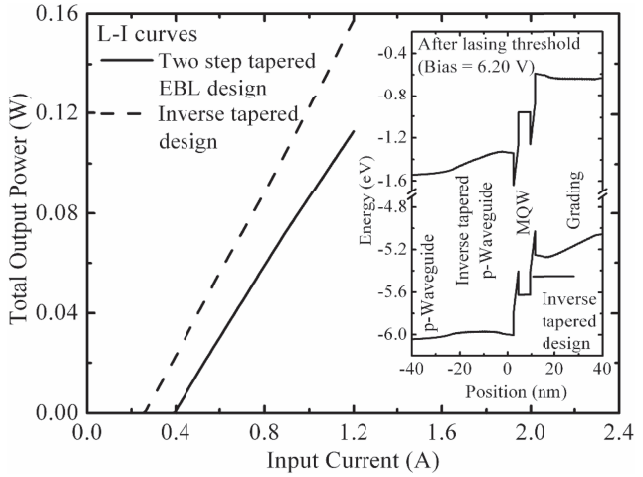

Fig. 11. Comparison of L-I curves between two step tapered and inverse tapered designs. Inverse tapering reduces threshold current by 33% and improves slope efficiency by 14%. Inset shows the energy band diagram of the inverse tapered design above the lasing threshold, and the clear absence of potential barriers to hole injection.

leakage within tolerable limits via appropriate selection of MQW (and spacer) material compositions.

We therefore modify baseline design of Table I by replacing the tapered EBL with an inverse tapered p-waveguide layer (from $Al_{0.54}GaN$ to $Al_{0.48}GaN$). Inverse tapering is affected over a thickness of 20 nm, with all other quantities unchanged. Simulation results show that the parasitic electrostatic barrier to hole injection is suppressed significantly (see Fig. 10). Excellent hole injection efficiency leads to the dramatic improvement in LD performance shown in Fig. 11. The L-I characteristic of two step tapered EBL design is included for comparison. The proposed inverse tapered design's threshold current is reduced by 33% and slope efficiency is improved by 14% with respect to the two step tapered EBL design. Threshold voltage is also reduced by 0.4 V (results not shown here). As there is no explicit EBL in the inverse tapered design, leakage of electrons from the active region can only be kept within acceptable limits if MQW and spacer compositions are chosen judiciously. To investigate this, we have studied

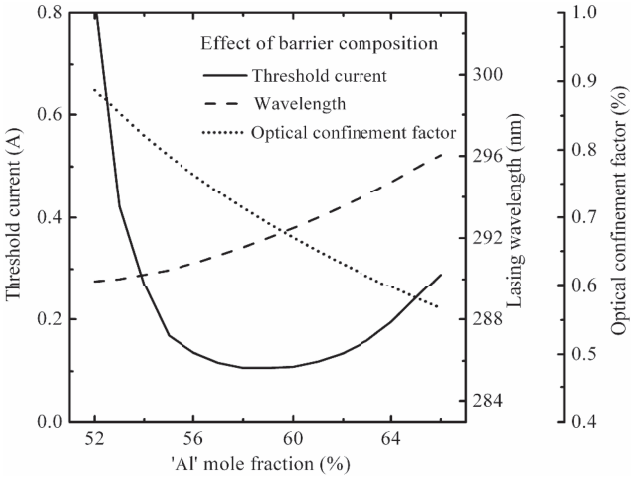

Fig. 12. Effect of QWBs and spacer's composition on the threshold current, lasing wavelength and optical confinement factor. Narrow bandgap barriers fail to block electron leakage. On the contrary, wider bandgap QWBs (and spacer) pushes the optical mode downwards and red-shits emission wavelength via quantum-confined stark effect (QCSE).

the influence of different spacer compositions on the inverse-tapered design described. The material composition of the QWBs are kept identical to that of the spacer to ensure similar emission wavelength among the QWs. Fig. 12 shows how the threshold current, lasing wavelength and optical confinement factor change with spacer (and QWB) composition. Rapid degradation of threshold current indicates that electron leakage becomes dominant if the aluminum content falls below 54%. 59% Al minimizes the threshold current (and electron leakage), incurring a small red-shift to the emission wavelength. The red-shift can be easily corrected by modifying QWs' composition and/or thickness. For aluminum content in excess of 60%, threshold current starts rising sharply because of degradation of optical confinement and further separation of electron and hole wavefunctions within the QWs.

Many researchers have proposed different approaches for improving the conductivity of p-type layers, hole injection efficiency and electrical confinement of carriers inside the active region in LDs and LEDs operating within the visible and UV spectrum. Several articles are cited in Satter *et al*. [2] which report new strategies for reduction of the high activation energy of Mg dopants or the increase of free hole concentration in III-N materials. A technique known as "polarization doping" has been suggested for the improvement of p-type dopant (Mg) ionization efficiency in compositionally graded AlGaN layers through the field ionization of the dopant atoms via the electric field induced by polarization charge [4], [9], [33]–[37]. This appellation is somewhat misleading, as electric fields of sufficient magnitude to ionize deep acceptor atoms would necessarily drive free carriers away from the high-field region, leaving behind only fixed space charge rather than highly conductive material. Instead, compositional grading can volumetrically redistribute sufficient negative polarization charge to make it energetically favorable for free holes in adjacent material to drift or diffuse into the compositionally graded region, thereby creating a high free hole density irrespective of whether Mg atoms are electrically active. Both N-face [4], [9], [33], [36] and the conventional metal-face [34], [35], [37] growth can benefit from compositional grading, producing a flat and smooth valence band profile right up to the edge of the active region to ensure superlative hole injection efficiency. If N-face growth is adopted, one must not only ensure good crystalline quality of the epitaxial layers, but also make Ohmic contact to a wide bandgap p-type layer [35].

Several authors have reported short-period superlattices (SPSL) based EBLs [38], [39] to improve hole injection efficiency and electrical confinement of electrons. Although this strategy effectively reduces hole blocking barrier height, it also directly introduces deep hole traps which impede the vertical transport of holes through these layers. Lattice matched ternary AlInN [40] and polarization charge matched (partial) quaternary AlInGaN EBLs [41] have also been used to improve hole injection efficiency and electrical confinement of electrons. From the growth perspective, one of the most attractive features of our proposed inverse tapered design is that it is an all AlGaN based design and it does not critically depend on the polarization charge matching via precise control of quaternary compositions. Surely, the design can be improved further if properly chosen quaternaries are used for QWBs, spacer and EBL layers. Although the precise control and crystalline growth of AlInGaN compositions may be difficult, the issues do not appear to be fundamental.

Explicit consideration of optical losses associated with sub-bandgap absorption in the epitaxial structure of Table I quantitatively degrade both threshold current and slope efficiency (results not presented here), consistent with expectations. These simulations also confirm, however, that the inverse taper design not only continues to provide the best performance among the three designs studied, but is also substantially more robust to optical loss than the other two designs considered.

IV. Conclusion

A prototypical 290 nm DUV edge emitting LD design based on AlGaN ternary materials has been presented. Conventionally tapered EBLs have been identified as the origin of a large electrostatic barrier to hole injection, associated with unscreened polarization charge. Numerical simulations indicate that properly designed inverse tapered p-waveguide layers can significantly improve threshold current and slope efficiency through elimination of barriers to vertical hole transport, while incurring a minimum penalty to electron leakage from the active region. Optically transparent but narrow bandgap material has been utilized for n-waveguide layers to reduce the optical absorption in lossy p-Ohmic metal by pulling the optical mode downward. The proposed inverse tapered structure can be easily extended to LD designs operating at shorter wavelengths.

References

[1] P. J. Parbrook and T. Wang, "Light emitting and laser diodes in the ultraviolet," *IEEE J. Sel. Topics Quantum Electron.*, vol. 17, no. 5, pp. 1402–1411, Sep./Oct. 2011.

[2] M. M. Satter, Z. Lochner, J. H. Ryou, S. C. Shen, R. D. Dupuis, and P. D. Yoder, "Polarization matching in AlGaN-based multiple-quantum-well deep ultraviolet laser diodes on AlN substrates using quaternary AlInGaN barriers," *J. Lightw. Technol.*, vol. 30, no. 18, pp. 3017–3025, Sep. 15, 2012.

[3] T. Wunderer, C. L. Chua, J. E. Northrup, Z. Yang, N. M. Johnson, M. Kneissl, *et al.*, "Optically pumped UV lasers grown on bulk AlN substrates," *Phys. Status Solidi (c)*, vol. 9, nos. 3–4, pp. 822–825, 2012.
[4] J. Piprek, "Ultra-violet light-emitting diodes with quasi acceptor-free AlGaN polarization doping," *Opt. Quantum Electron.*, vol. 44, nos. 3–5, pp. 67–73, 2011.
[5] A. A. Allerman, M. H. Crawford, A. J. Fischer, K. H. A. Bogart, S. R. Lee, D. M. Follstaedt, *et al.*, "Growth and design of deep-UV (240-290 nm) light emitting diodes using AlGaN alloys," *J. Cryst. Growth*, vol. 272, nos. 1–4, pp. 227–241, 2004.
[6] M. Shatalov, A. Lunev, X. Hu, O. Bilenko, I. Gaska, W. Sun, *et al.*, "Performance and applications of deep UV led," *Int. J. High Speed Electron. Syst.*, vol. 21, no. 1, pp. 1250011-1–1250011-15, 2012.
[7] S. Majety, J. Li, X. K. Cao, R. Dahal, B. N. Pantha, J. Y. Lin, *et al.*, "Epitaxial growth and demonstration of hexagonal BN/AlGaN p-n junctions for deep ultraviolet photonics," *Appl. Phys. Lett.*, vol. 100, no. 6, pp. 061121-1–061121-4, 2012.
[8] D. A. Haeger, E. C. Young, R. B. Chung, F. Wu, N. A. Pfaff, M. Tsai, *et al.*, "384-nm laser diode grown on a (2021) semipolar relaxed AlGaN buffer layer," *Appl. Phys. Lett.*, vol. 100, no. 6, pp. 161107-1–161107-4, 2012.
[9] J. Verma, J. Simon, V. Protasenko, T. Kosel, H. G. Xing, and D. Jena, "N-polar III-nitride quantum well light-emitting diodes with polarization-induced doping," *Appl. Phys. Lett.*, vol. 99, no. 17, p. 171104, 2011.
[10] S. Hwang, D. Morgan, A. Kesler, M. Lachab, B. Zhang, A. Heidari, *et al.*, "276 nm substrate-free flip-chip AlGaN light-emitting diodes," *Appl. Phys. Exp.*, vol. 4, no. 3, p. 032102, 2011.
[11] M. M. Satter, H. J. Kim, Z. Lochner, J. H. Ryou, S. C. Shen, R. D. Dupuis, *et al.*, "Design and analysis of 250-nm AlInN laser diodes on AlN substrates using tapered electron blocking layers," *IEEE J. Quantum Electron.*, vol. 48, no. 5, pp. 703–711, May 2012.
[12] M. L. Nakarmi, N. Nepal, J. Y. Lin, and H. X. Jiang, "Photoluminescence studies of impurity transitions in Mg-doped AlGaN alloys," *Appl. Phys. Lett.*, vol. 94, no. 9, pp. 091903-1–091903-3, 2009.
[13] M. Imura, N. Kato, N. Okada, K. Balakrishnan, M. Iwaya, S. Kamiyama, *et al.*, "Mg-doped high-quality $Al_xGa_{1-x}N$ (x=0-1) grown by high-temperature metal-organic vapor phase epitaxy," *Phys. Status Solidi (c)*, vol. 4, no. 7, pp. 2502–2505, 2007.
[14] S.-N. Lee, J. Son, T. Sakong, W. Lee, H. Paek, E. Yoon, *et al.*, "Investigation of optical and electrical properties of Mg-doped p-$In_xGa_{1-x}N$, p-GaN and p-$Al_yGa_{1-y}N$ grown by MOCVD," *J. Cryst. Growth*, vol. 272, pp. 455–459, Dec. 2004.
[15] K. B. Nam, M. L. Nakarmi, J. Li, J. Y. Lin, and H. X. Jiang, "Mg acceptor level in AlN probed by deep ultraviolet photoluminescence," *Appl. Phys. Lett.*, vol. 83, no. 5, pp. 878–880, Aug. 2003.
[16] Y.-Y. Zhang and G.-R. Yao, "Performance enhancement of blue light-emitting diodes with AlGaN barriers and a special designed electron-blocking layer," *J. Appl. Phys.*, vol. 110, no. S1, p. 093104, 2011.
[17] W. Yang, D. Li, N. Liu, Z. Chen, L. Wang, L. Liu, *et al.*, "Improvement of hole injection and electron overflow by a tapered AlGaN electron blocking layer in InGaN-based blue laser diodes," *Appl. Phys. Lett.*, vol. 100, no. 3, pp. 031105-1–031105-5, 2012.
[18] S.-J. Lee, C.-Y. Cho, S.-H. Hong, S.-H. Han, S. Yoon, S.-T. Kim, *et al.*, "Enhanced optical power of InGaN/GaN light-emitting diode by AlGaN interlayer and electron blocking layer," *IEEE Photon. Technol. Lett.*, vol. 24, no. 22, pp. 1991–1994, Nov. 15, 2012.
[19] Y. K. Kuo, J. Y. Chang, and M. C. Tsai, "Enhancement in hole-injection efficiency of blue InGaN light-emitting diodes from reduced polarization by some specific designs for the electron blocking layer," *Opt. Lett.*, vol. 35, pp. 3285–3287, Oct. 2010.
[20] M. M. Satter and P. D. Yoder, "Lateral carrier confinement and threshold current reduction in InGaN QW lasers with deeply etched mesa," *Opt. Quantum Electron.*, vol. 42, pp. 747–754, Oct. 2011.
[21] R. F. Pierret, *Advanced Semiconductor Fundamentals*, 2nd ed. Upper Saddle River, NJ, USA: Prentice-Hall, 2003.
[22] J. Piprek, *Nitride Semiconductor Devices: Principles and Simulation*. New York, NY, USA: Wiley, 2007.
[23] J. Piprek, *Semiconductor Optoelectronic Devices: Introduction to Physics and Simulation*. San Diego, CA, USA: Academic Press, 2003.
[24] E. Kioupakis, P. Rinke, and C. G. V. D. Walle, "Determination of internal loss in nitride lasers from first principles," *Appl. Phys. Exp.*, vol. 3, p. 082101, Jul. 2010.
[25] C.-Y. Huang, Y.-D. Lin, A. Tyagi, A. Chakraborty, H. Ohta, J. S. Speck, *et al.*, "Optical waveguide simulations for the optimization of InGaN-based green laser diodes," *J. Appl. Phys.*, vol. 107, p. 023101, Jan. 2010.
[26] M. Kuramoto, C. Sasaoka, N. Futagawa, M. Nido, and A. A. Yamaguchi, "Reduction of internal loss and threshold current in a laser diode with a ridge by selective re-growth (RiS-LD)," *Phys. Status Solidi (a)*, vol. 192, p. 329, Apr. 2002.
[27] M. Polyanskiy. (2013, Jan. 20). *Refractive Index Database* [Online]. Available: http://refractiveindex.info
[28] J. R. Chen, T. S. Ko, P. Y. Su, T. C. Lu, H. C. Kuo, Y. K. Kuo, *et al.*, "Numerical study on optimization of active layer structures for GaN/AlGaN multiple-quantum-well laser diodes," *J. Lightw. Technol.*, vol. 26, pp. 3155–3165, Sep. 1, 2008.
[29] F. Bertazzi, M. Goano, and E. Bellotti, "A numerical study of Auger recombination in bulk InGaN," *Appl. Phys. Lett.*, vol. 97, no. 23, pp. 231118-1–231118-3, 2010.
[30] P. Kozodoy, H. Xing, S. P. DenBaars, U. K. Mishra, A. Saxler, R. Perrin, *et al.*, "Heavy doping effects in Mg-doped GaN," *J. Appl. Phys.*, vol. 87, no. 4, pp. 1832–1835, 2000.
[31] K. Kumakura, T. Makimoto, and N. Kobayashi, "Mg-acceptor activation mechanism and transport characteristics in p-type InGaN grown by metalorganic vapor phase epitaxy," *J. Appl. Phys.*, vol. 93, no. 6, p. 3370, 2003.
[32] T. Katsuno, Y. Liu, D. Li, H. Miyake, K. Hiramatsu, T. Shibata, *et al.*, "n-type conductivity control of AlGaN with high Al mole fraction," *Phys. Status Solidi (c)*, vol. 3, no. 6, pp. 1435–1438, 2006.
[33] J. Simon, V. Protasenko, C. Lian, H. Xing, and D. Jena, "Polarization-induced hole doping in wide-band-gap uniaxial semiconductor heterostructures," *Science*, vol. 327, no. 5961, pp. 60–64, 2009.
[34] L. Zhang, K. Ding, N. X. Liu, T. B. Wei, X. L. Ji, P. Ma, *et al.*, "Theoretical study of polarization-doped GaN-based light-emitting diodes," *Appl. Phys. Lett.*, vol. 98, no. 10, pp. 101110-1–101110-3, 2011.
[35] L. Zhang, K. Ding, J. C. Yan, J. X. Wang, Y. P. Zeng, T. B. Wei, *et al.*, "Three-dimensional hole gas induced by polarization in (0001)-oriented metal-face III-nitride structure," *Appl. Phys. Lett.*, vol. 97, no. 6, p. 062103, 2010.
[36] K. Dong, D. Chen, B. Liu, H. Lu, P. Chen, R. Zhang, *et al.*, "Characteristics of polarization-doped N-face III-nitride light-emitting diodes," *Appl. Phys. Lett.*, vol. 100, no. 7, pp. 073507-1–073507-3, 2012.
[37] S. Li, M. E. Ware, V. P. Kunets, M. Hawkridge, P. Minor, J. Wu, *et al.*, "Polarization induced doping in graded AlGaN films," *Phys. Status Solidi (c)*, vol. 8, nos. 7–8, pp. 2182–2184, 2011.
[38] Y. Y. Zhang and Y. A. Yin, "Performance enhancement of blue light-emitting diodes with a special designed AlGaN/GaN superlattice electron-blocking layer," *Appl. Phys. Lett.*, vol. 99, no. 1, p. 221103, 2011.
[39] Y.-Y. Zhang, X.-L. Zhu, Y.-A. Yin, and J. Ma, "Performance enhancement of near-UV light-emitting diodes with an InAlN/GaN superlattice electron-blocking layer," *IEEE Electron Device Letters*, vol. 33, no. 7, pp. 994–996, Jul. 2012.
[40] S. Choi, M. H. Ji, J. Kim, H. J. Kim, M. M. Satter, P. D. Yoder, *et al.*, "Efficiency droop due to electron spill-over and limited hole injection in III-nitride visible light-emitting diodes employing lattice-matched InAlN electron blocking layers," *Appl. Phys. Lett.*, vol. 101, p. 161110, Oct. 2012.
[41] Y.-K. Kuo, Y.-H. Chen, J.-Y. Chang, and M.-C. Tsai, "Numerical analysis on the effects of bandgap energy and polarization of electron blocking layer in near-ultraviolet light-emitting diodes," *Appl. Phys. Lett.*, vol. 100, no. 4, pp. 043513-1–043513-3, 2012.

Md. Mahbub Satter received the B.Sc. and M.Sc. degrees in electrical and electronic engineering from the Bangladesh University of Engineering and Technology (BUET), Dhaka, Bangladesh, in 2005 and 2008, respectively. He is currently pursuing the Ph.D. degree with the Georgia Institute of Technology, Atlanta, focusing in the area of semiconductor photonic devices.

He was a Lecturer with the Department of Electrical and Electronic Engineering, BUET, from 2005 to 2009.

Zachary Lochner (S'03) was born in Buffalo, NY, USA. He received the B.S. degree in electrical engineering from the University at Buffalo, Buffalo, in 2007, and the M.S. and Ph.D. degrees in electrical engineering from the Georgia Institute of Technology, Atlanta, in 2010 and 2013, respectively.

Tsung-Ting Kao received the B.S. and M.S. degrees from National Chiao-Tung University in 2004 and 2006, respectively. He has been pursuing the Ph.D. degree with the Georgia Institute of Technology, Atlanta, since 2008.

Yuh-Shiuan Liu received the B.S. degree in electrical engineering from the University of Illinois at Urbana-Champaign in 2012. He is currently pursuing the Ph.D. degree with the Center for Compound Semiconductors, Georgia Institute of Technology, Atlanta.

Xiao-Hang Li received the B.S. degree in applied physics from the Huazhong University of Science and Technology in 2008. He is currently pursuing the Ph.D. degree with the Center for Compound Semiconductors, Georgia Institute of Technology, Atlanta, and was recognized in 2013 with the SPIE D. J. Lovell Scholarship.

Shyh-Chiang Shen (M'01–SM'06) was born in Taipei, Taiwan, in 1971. He received the B.S.E.E. and M.S.E.E. degrees from National Taiwan University, Taipei, in 1993 and 1995, respectively, and the Ph.D. degree in electrical engineering from the University of Illinois at Urbana-Champaign, Urbana, in 2001. He joined the faculty of the Georgia Institute of Technology, Atlanta, in 2005.

Russell D. Dupuis (SM'84–F'87) received the B.S., M.S., and Ph.D. degrees in electrical engineering from the University of Illinois at Urbana-Champaign, Urbana. He was with Texas Instruments Inc., Dallas, from 1973 to 1975. In 1975, he joined Rockwell International, Anaheim, CA, USA, where he was the first to demonstrate that metalorganic chemical vapor deposition (MOCVD) could be used for the growth of high-quality semiconductor thin films and devices. In 1979, he joined the AT&T Bell Laboratories, Murray Hill, NJ, USA, where he extended his work to the growth of InP-InGaAsP by MOCVD. In 1989, he became a Chair Professor of electrical and computer engineering with the University of Texas, Austin. In 2003, he was a Chair Professor of electrical and computer engineering and materials science and engineering with the School of Electrical and Computer Engineering, Georgia Institute of Technology, Atlanta. He currently holds the Steve W. Chaddick Endowed Chair in electro-optics and is a Georgia Research Alliance Eminent Scholar. He is a member of the National Academy of Engineering, the American Physical Society, and the Optical Society of America. He was the recipient of many awards and distinctions throughout his career, including the National Medal of Technology in 2002, the John Bardeen Award of the Minerals, Metals and Materials Society in 2003, and the IEEE Edison Medal in 2007.

P. D. Yoder (M'88–SM'05) received the B.S.E.E. degree from Cornell University, Ithaca, NY, USA, in 1990, and the M.S. and Ph.D. degrees from the University of Illinois at Urbana-Champaign, Urbana, in 1991 and 1993, respectively. He was a Post-Doctoral Research Associate with the Swiss Federal Institute of Technology, Zurich, Switzerland, in 1993. He was a Member of Technical Staff with the Bell Laboratories, Murray Hill, NJ, USA, and Agere Systems, Murray Hill. He joined the faculty of the Georgia Institute of Technology, Atlanta, in 2003.